Strongly Scattering Medium Along Slow Earthquake Fault Zones Based on New Observations of Short-Duration Tremors

A. Toh, Yann Capdeville, W.-C. Chi, S. Ide

Geophysical Research Letters

RESEARCH LETTER
10.1029/2022GL101851

Strongly Scattering Medium Along Slow Earthquake Fault Zones Based on New Observations of Short-Duration Tremors

A. Toh[1], Y. Capdeville[2], W.-C. Chi[3], and S. Ide[1]

[1]Department of Earth and Planetary Science, University of Tokyo, Tokyo, Japan, [2]Laboratoire de Planétologie et de Géodynamique, Université de Nantes, Nantes, France, [3]Institute of Earth Sciences, Academia Sinica, Taipei, Taiwan

Key Points:

- Short-duration tremors in ocean-bottom seismometer records suggest that the source process of tremors is not always long
- Short-duration tremors can be interpreted by placing a strongly scattering medium around their source
- Such a medium embedded along the slow earthquake fault zone could play a key role in the tremor source process

Supporting Information:

Supporting Information may be found in the online version of this article.

Correspondence to:

A. Toh,
akiko.toh@eps.s.u-tokyo.ac.jp

Citation:

Toh, A., Capdeville, Y., Chi, W.-C., & Ide, S. (2023). Strongly scattering medium along slow earthquake fault zones based on new observations of short-duration tremors. *Geophysical Research Letters*, *50*, e2022GL101851. https://doi.org/10.1029/2022GL101851

Received 8 NOV 2022
Accepted 10 APR 2023

Author Contributions:

Conceptualization: A. Toh, Y. Capdeville, S. Ide
Formal analysis: A. Toh
Funding acquisition: A. Toh, W.-C. Chi, S. Ide
Methodology: A. Toh, Y. Capdeville
Software: Y. Capdeville
Writing – original draft: A. Toh
Writing – review & editing: A. Toh, Y. Capdeville, W.-C. Chi, S. Ide

Abstract Tremors are a type of slow earthquake with long-duration signals compared to ordinary earthquakes. The long signals have been considered to solely reflect their long source process. However, here, we provide evidence suggesting that the source processes of tremors are not always long. We refer to these observations as short-duration tremors. They were recorded by ocean-bottom seismometers placed very close to the source. Although these tremors exhibit a short-duration signal when recorded near the source, they exhibit a typical long-duration signal elsewhere. Our numerical simulations demonstrate that the features can be captured by considering a strongly scattering medium around their source. One such structure could be small low-velocity inclusions distributed around the seismic source. The inclusions may represent the seismic expression of geologically detected aquifers in tremor source regions. Furthermore, this medium could be embedded along the slow earthquake fault zone and play a critical role in their source process.

Plain Language Summary At least two types of earthquakes occur in shallow subduction zones: ordinary earthquakes and tremors. Tremors are known to exhibit long signal duration compared to ordinary earthquakes. To date, tremors' long-duration signal has been solely interpreted by their source process. Here, we discovered tremors that exhibit short duration signals when recorded close from the source which we referred to as "short-duration tremors". They suggest that tremors' source process is not always long and structural effects may partially form the typical long-duration signals. We performed numerical simulations on elastic wave propagation and demonstrated that the observations can be qualitatively reproduced by assuming a strongly scattering material surrounding the seismic source. On the other hand, it has been reported based on ocean bottom drilling project that tremor source region may consist of patchily distributed aquifers. The inclusions in our model may be the seismic expressions of the geologically detected aquifers. Further, such a structure could be embedded along the slow-earthquake fault zone and play a key role in their source process.

1. Introduction

At least two types of earthquakes occur in shallow subduction zones: ordinary earthquakes and tremors (Beroza & Ide, 2011). Compared to ordinary earthquakes of similar magnitude, tremor signals are characterized by a (a) long duration, (b) unclear onset, and (c) depletion of seismic energy above 10 Hz (Obana & Kodaira, 2009). Tremors are a type of slow-earthquake observed in a wide spectrum, whose duration and magnitude follow a different scaling law compared to ordinary earthquakes (Ide et al., 2007). However, the cause of these differences remains a fundamental question in seismology.

To date, the waveform differences between ordinary earthquakes and tremors have been solely attributed to seismic source processes (e.g., Ide, 2008; Im & Avouac, 2021; Sibson, 2017). Often, the tremors' long-duration signal has been interpreted by a successive occurrence of small and slow shear-slips distinguished as low-frequency earthquakes (LFEs, Shelly et al., 2007, Figure 1d). The interpretations were based on observations of deep tremors (>15 km) recorded by land-based seismographs (Ide, 2012). On the other hand, geophysical and geological surveys collectively suggest the presence of overpressured fluids in the tremor source region, which are considered a cause of tremors (Bürgmann, 2018; Saffer & Wallace, 2015). Nevertheless, no consensus has been reached regarding how the fluids cause the two seismic phenomena to differ. Furthermore, although ample fluids around the source may influence seismic wave propagation and distort waveforms by scattering, such structural effects have not been investigated in-depth.

Here, we present evidence of tremors exhibiting short-duration signals at stations close to the source. Our observations suggest that the source process of tremors is not necessarily long and that long-duration signals may be

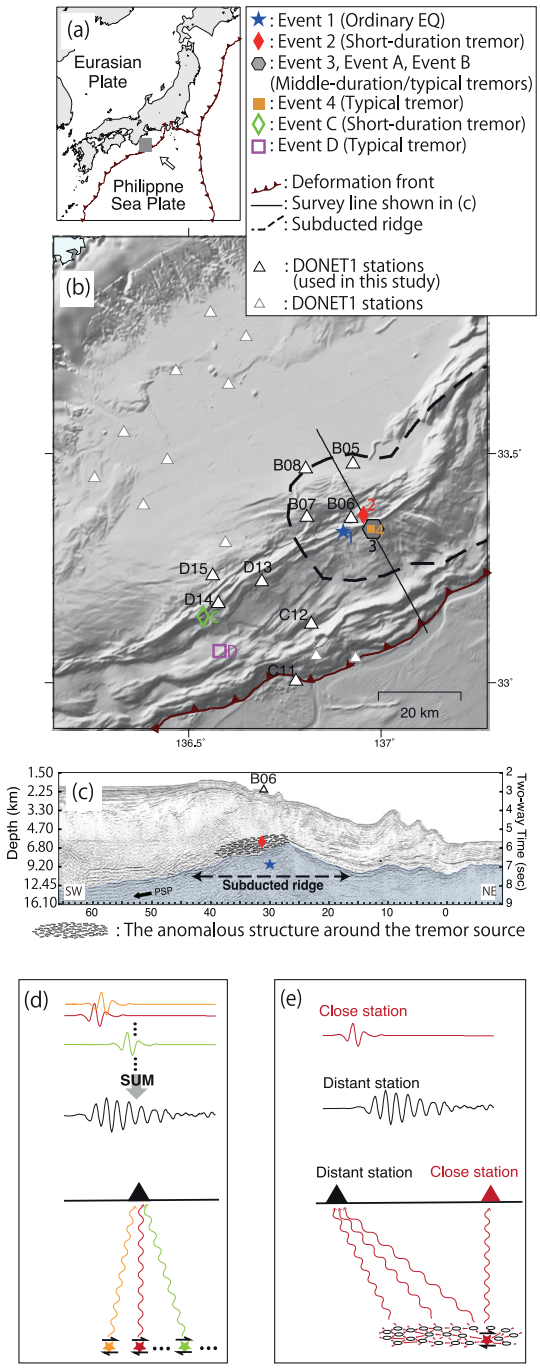

Figure 1. (a) Location of the study area. (b) Station locations of DONET1 and estimated epicenters of seismic events. The epicenters of Events 1 and D were estimated using an envelope correlation method (ECM; Ide, 2012) by assuming a 1D Vs structure (Ueno et al., 2002). The epicenters of Events 2, 3, 4, A, B, and C were obtained by Toh et al. (2018). (c) Hypocenters estimated for Event 1 (blue star) and Event 2 (red diamond) are plotted along a cross-section (Park et al., 2003). The anomalous structure inferred from the short-duration tremor is schematically illustrated. (d, e) Schematics on causes of tremors' prolonged signals for a previously proposed mechanism (Shelly et al., 2007) and our proposed mechanism.

partially formed by structural effects. The evidence was obtained thanks to ocean-bottom seismometers (OBSs) that record shallow tremors at unparalleled proximities. Numerical simulations on elastic wave propagations indicate that observations can be qualitatively reproduced by assuming a strongly scattering material surrounding the tremor source, which may be related to the above-mentioned fluid. Such a structure, potentially the slow earthquake fault zone, may play a crucial role in the slow earthquake source process.

2. Observations of Short-Duration Tremors

The waveforms of four seismic events (Events 1–4) obtained by broadband OBSs of DONET1 (Aoi et al., 2020; Kaneda et al., 2015) (Figure 1) in the Nankai Trough are presented in Figure 2. All four events are located close to station B06 and can be assessed based on the moveout times of the arriving signals. Among the four events, Events 1 and 4 represent a typical ordinary earthquake and tremor. The ordinary earthquake exhibits a short-duration signal of 2–5 s throughout the network, as plotted in Figure 3. In contrast, the typical tremor exhibits long-duration signals (>20 s) at all stations as well as unclear signal onsets and depletion in the high-frequency components (Figure 2d). In contrast, the tremor represented as Event 2 in Figure 2 exhibits a signal of 3.4 s at the closest station B06, which is nearly as short as an ordinary earthquake's duration, however, the duration becomes longer (>10 s) resembling that of a typical tremor at stations beyond B06. Furthermore, the onset of P arrival is identified at B06 for Event 2, which is unusual for tremors. Hereafter, we refer to this type of tremor as a "short-duration tremor." Indeed, observations of short-duration tremors are not rare and can be found in other regions below DONET1. One example near station D14 is Event C presented in Figure S2 (Supporting Information S1).

The depth of the ordinary earthquake (Event 1) and short-duration tremor (Event 2) presented in Figure 1c were estimated based on S-P differential travel times observed at station B06, which were ∼2.8 and ∼1.8 s, respectively. We used a P-wave velocity (Vp) profile near station B06 (Kamei et al., 2012) and set the Vp to S-wave velocity (Vs) ratio to 2. The plate boundary is located at a depth of ∼5 km (Park et al., 2003). Assuming that the epicenters of Event 1 and Event 2 are located within 8 and 5 km of B06, respectively, their depths are estimated to be 9–12 km and 4–5 km beneath the seafloor. These estimates are consistent with those of previous studies, which concluded that ordinary earthquakes and tremors in this region occur below and above the plate boundary, respectively (Nakano et al., 2015; Sugioka et al., 2012; To et al., 2015).

Although the waveforms of the short-duration tremors at the closest station resemble those of ordinary earthquakes, they are classified as tremors due to the following two points. First, even when the signal duration is short, the high-frequency seismic energy is depleted (Figure 2b), which is a well-known feature of tremors. Second, the trends of the signal duration and maximum amplitude with respect to epicentral distance for the short-duration tremor resemble those of other tremors rather than ordinary earthquakes (Figure 3). For example, the maximum amplitude of all the tremors drops sharply at short epicentral distances, which differs from the fluctuating trend of the ordinary earthquake (Figure 3b).

Further, the signal durations plotted in Figure 3a infer that two different mechanisms may contribute to the prolonged tremor signals. The first involves the generation of duration variation observed among different tremors. For

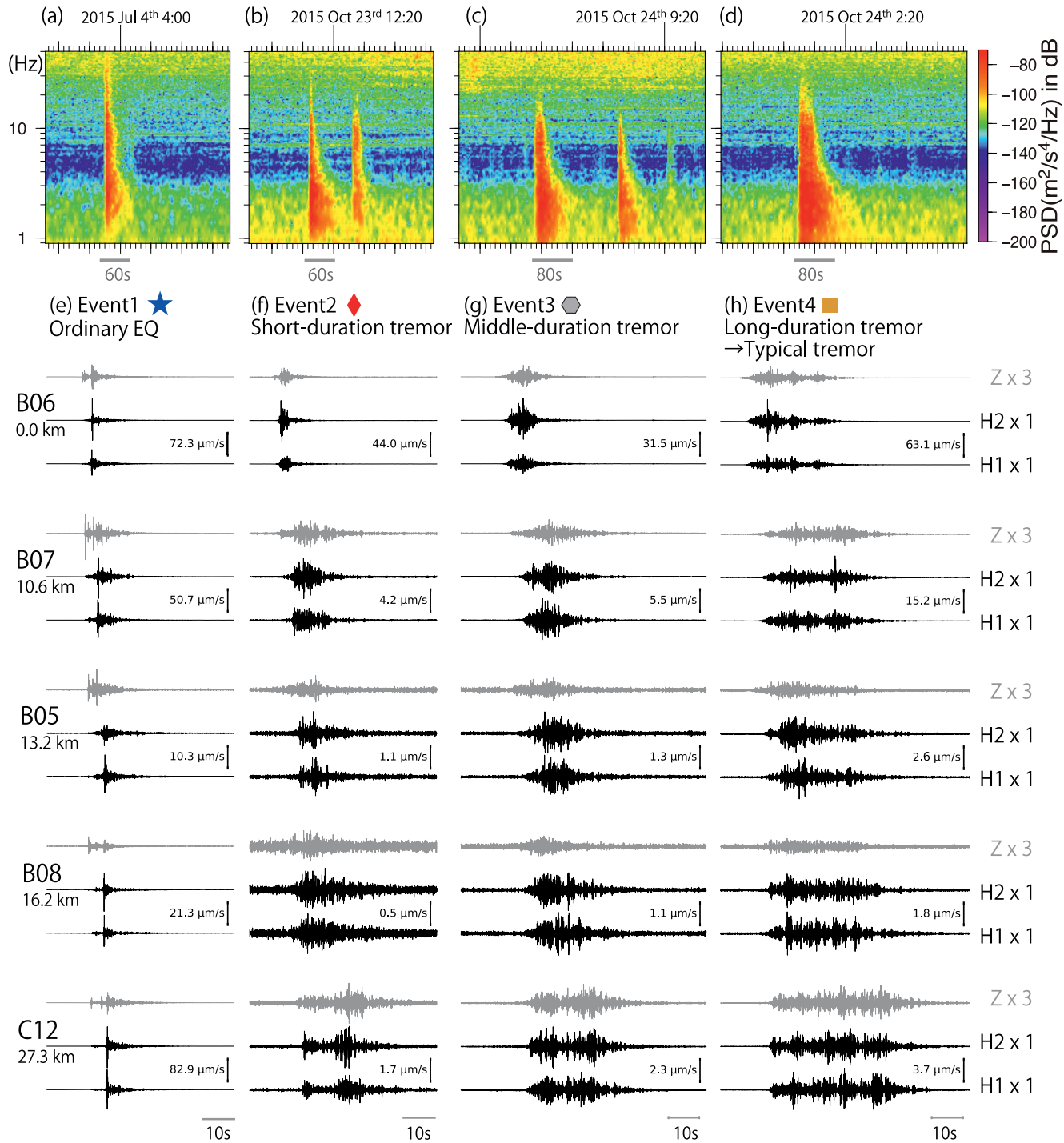

Figure 2. (a–d) Spectrograms of Events 1 to 4. The original data were recorded by Guralp CMG-3T seismographs. The instrument response was corrected. A horizontal component (H1) recorded at B06 is plotted for each event. The gray horizontal bars indicate the portions with waveforms plotted in (e–h). (e–h) Records at five stations close to station B06, filtered at 4–20 Hz. The epicentral distance from station B06 is indicated below each station name. The amplitude is normalized by the maximum amplitude per station. The vertical components are plotted as gray lines, amplified three times the horizontal ones. The radiated seismic energy was estimated to be 2.7×10^4, 1.5×10^4, 5.4×10^4, and 16.7×10^4 J for Events 1, 2, 3, and 4, respectively, using the methods described in Text S1 in Supporting Information S1.

example, the signal duration is 3.4 and 20.0 s at B06 for Events 2 and 4, respectively. Given the proximity of these tremors to B06, the duration difference is most readily explained by a source duration difference, as previously proposed. The second is an unknown mechanism that substantially prolongs the signal from the closest station

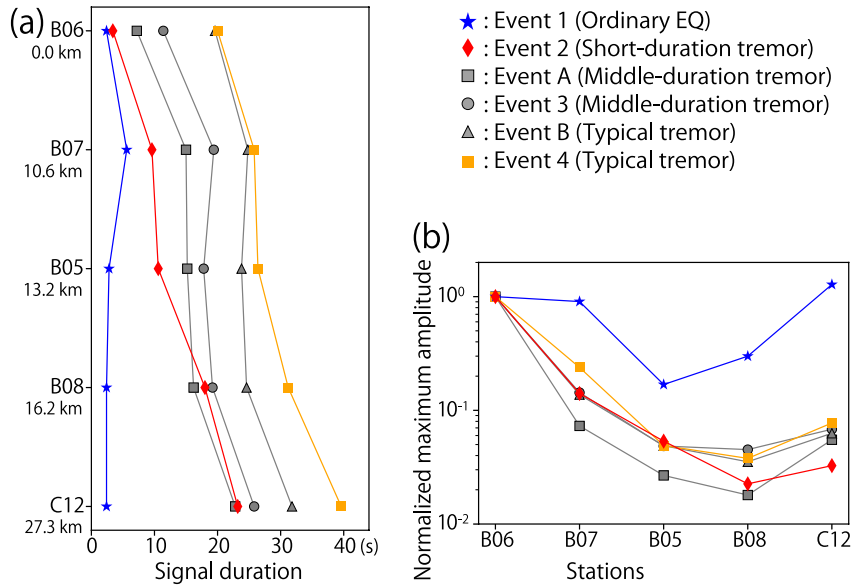

Figure 3. (a) Signal durations and (b) maximum amplitudes measured for six seismic events located close to B06. Measurements required the two horizontal components to first be filtered between 4 and 20 Hz; their root sum squares (RSS) were then low-pass filtered at 0.4 Hz. The durations were defined as the signal length at which the amplitude was larger than one-third of the maximum amplitude of each RSS trace. All RSS traces used for the measurements are plotted in Figure S1 in Supporting Information S1. The five tremors are labeled subjectively as short-duration, middle-duration, and typical tremors, depending on the signal duration at B06.

(B06) to the subsequent closest station (B07), located only ~10 km away. This feature is observed in all tremors but is most noticeable with the short-duration tremor (Event 2) as the duration becomes nearly three times longer from station B06 (<4 s) to B07 (>10 s). Indeed, the source process cannot explain this feature given that, should the source process be long, we would observe a long-duration signal throughout the network at all the station, which was not the case. Therefore, it is necessary to consider a new mechanism that produces the long-duration signal from a short-duration source process.

We propose a mechanism whereby an anomalous structure that prolongs seismic signals is horizontally spread around the seismic source. With this structure, seismic waves recorded closely above the source (B06 in Figure 2) should scarcely propagate through the structure, thus, causing the signal duration to remain short. Conversely, the structure would prolong the seismic waves emitted toward distant stations. That is, the waves would depart the source more horizontally and propagate through the structure for longer distances. Another constraint of the structure is that it should not significantly alter the waveforms of ordinary earthquakes located below it (e.g., Figure 2e). Our observations suggest that signals should remain short even when the seismic waves propagate through the anomalous structure to reach stations.

3. Waveform Modeling and Results

While many structures can be proposed to prolong seismic signals, we examined the structure shown in Figure 4a. We considered a 2-D (P-SV) elastodynamic model that was 30 km wide and 10 km high. All except the top boundary were absorbent (Festa & Vilotte, 2005). In the background, the seismic velocities increased linearly from top to bottom (Figure 4b). The anomalous structure was placed an area of 5,400 m wide and 195 m high, and the lower-right corner of which was set to 2,000 m from the right and 2,655 m from the top. It comprised 400 randomly placed diamond-shaped inclusions, the width and height of which were randomly set between 60–90 m and 8.7–13.0 m, respectively. The Vs inside the inclusions was set arbitrarily to 200 m/s corresponding to a ~88% reduction from the surroundings by assuming mud. The inclusions' Vp and density were the same as in their surroundings.

Elastic wave propagations were simulated using a 2-D spectral element program (Komatitsch & Vilotte, 1998). The seismic source was a point source with a horizontal shear-slip mechanism. The source-time function was a

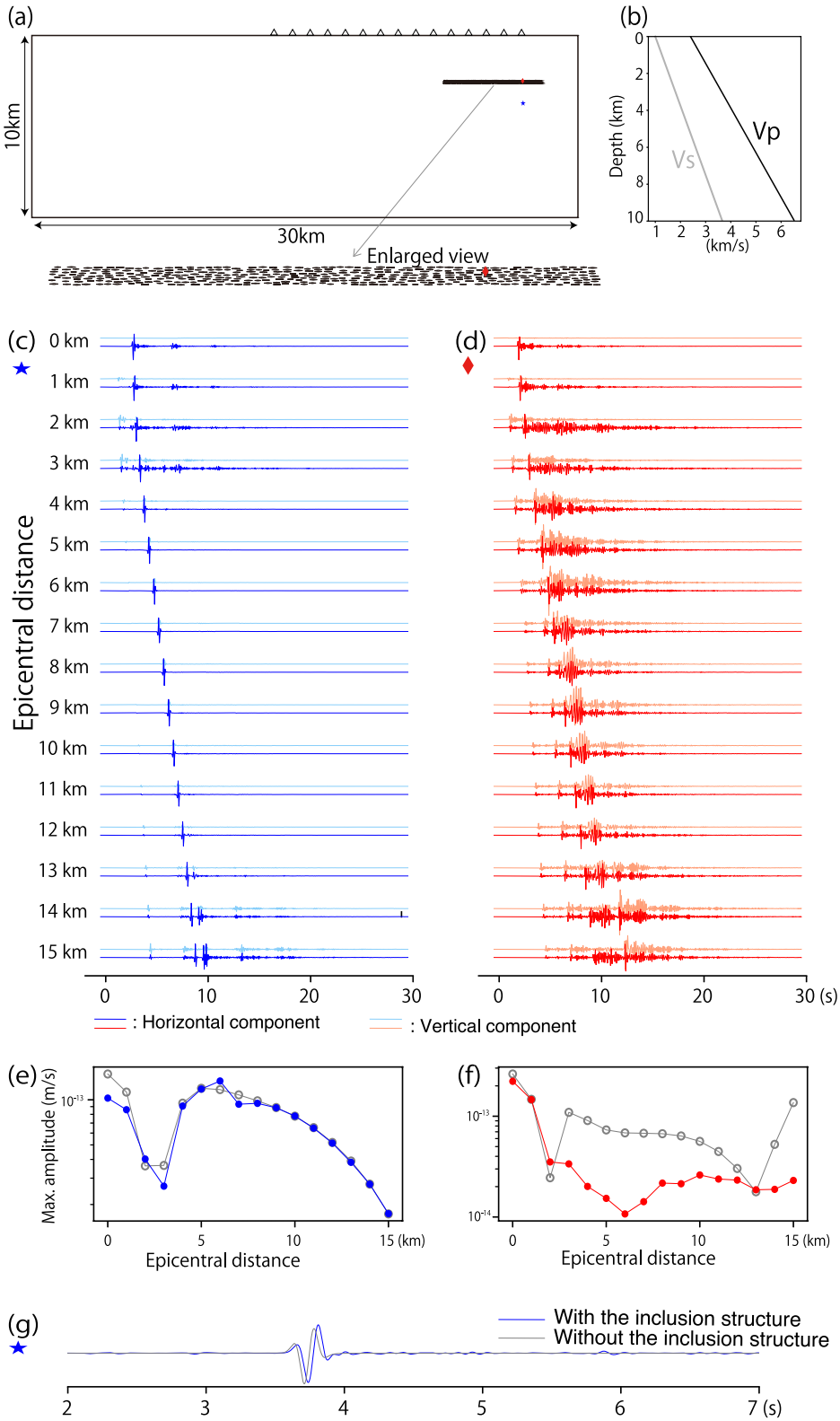

Figure 4.

Ricker wavelet with a central frequency of 5 Hz and a maximum frequency of ∼15 Hz. The mesh was designed to fit at least one element of degree 6 per minimum wavelength. That is, each quadrangular element comprised a grid of $(6 + 1)^2 = 49$ Gauss-Lobatto-Legendre points (Chaljub et al., 2007). The P and S wavelengths were approximately 680 and 340 m, respectively, at the depths of the distributed inclusions; thus, they were longer than the inclusions. Two simulations were performed. The first was with the source located between the inclusions at a depth of 2,510 m (red diamond in Figure 4a). The second was with the source located at a depth of 3,810 m (blue star in Figure 4a), corresponding to 1,155 m below the structure. They were both located 3,100 m from the right side of the entire domain. The receivers were placed on the top surface at a horizontal interval of 1 km. Finally, two additional simulations were performed to compare the source locations described above without the inclusions.

The synthetic waveforms obtained are plotted in Figures 4c and 4d, and they captured the features of the observed ordinary earthquakes and short-duration tremors, respectively. When the source was located inside (Figure 4d), the signal duration became longer at remote receivers (epicentral distance > ∼2 km) however remained short at the receiver above the source. Snapshots of the wavefield are presented in Figure S3 in Supporting Information S1. In contrast, the signal duration remained short when the source was located below, regardless of the epicentral distance (Figure 4c). The exceptionally long signal duration around the epicentral distance of 2–3 km was due to the nodal plane of the S-wave radiation pattern. Furthermore, when the source was located outside of the structure, the synthetic waveforms exhibited a phase shift of ∼0.05 s compared to the case without the distributed inclusions (Figure 4g), suggesting that the waves "perceive" the distributed inclusions as a low-velocity layer. Finally, the changes in the maximum amplitude with respect to the epicentral distance (Figures 4e and 4f) also captured the observed features shown in Figure 3b. When the source was located outside the structure, the maximum amplitude pattern (blue circles) followed that obtained without the structure (gray circles). Their fluctuations reflect the S-wave radiation pattern at the source. In contrast, when the source was inside the structure, the maximum amplitude decreased sharply near the epicenter (red circles).

4. Discussion

Our observations and modeling indicate that the long signal duration of tremors is not caused exclusively by the source process (e.g., Figure 1d) but also by an anomalous structure surrounding the source (Figure 1e). Given that the examined structural model is just a proposal, certain structures may cause more complex scatterings or resonance (e.g., Zhao et al., 2016). Also, a heterogeneous background model, such as proposed for the accretionary prism, may cause additional scatterings (Takemura et al., 2020). Herein, we analyzed the sensitivity of certain parameters, which can be summarized in three main points (Text S2 and Figures S4–S6 in Supporting Information S1). First, the inclusions must be small so that seismic waves emitted from the source below the structure do not become markedly altered (Figure S4 in Supporting Information S1). Second, the extended signal occurs only when inclusions are positioned very close to the seismic source, within the minimum wavelength (Figure S5 in Supporting Information S1). Third, when the seismic source is within the structure, slight shifts in its location (tens of meters) can significantly alter the synthetic waves (Figure S6 in Supporting Information S1). Although the effects of anelasticity were not considered in this study, our results in which the distributed inclusions prolong the signal should remain similar.

The discovery of short-duration tremors raises the question of whether tremors could represent phenomena with a source process like ordinary earthquakes, but located inside a specific structure. In the modeling, we used the same source time function for cases inside and outside the structure solely to investigate the wave propagation effects. Based on our observations, one possible scenario is that the source process becomes altered in such a way that differs from that of ordinary earthquakes by being located inside the structure. This speculation is based on certain features of tremors that our structural model cannot explain yet could be better understood if attributed to the source process. One such feature is the long signal duration of tremors, which persists even when recorded

Figure 4. (a) 2D structural model. The locations of seismic sources with synthetic waveforms shown in Panels (c and d) are plotted using a blue star and red diamond, respectively. The stations are shown by triangles. (b) Profiles of seismic velocities used in the background. (c, d) Synthetic waveforms for the source placed below the distributed inclusions and placed between the inclusions. The waveforms are normalized by the maximum amplitude per station. (e, f) The maximum amplitudes of the horizontal component are plotted with respect to the epicentral distance for the source placed outside (blue circles) and inside (red circles) the structure and without inclusions (gray circles). (g) Comparison of synthetic waveforms calculated with (blue line) and without (gray line) the distributed inclusions for the source below the structure. The horizontal component at an epicentral distance of 4 km is plotted for each case.

close to the seismic source. For instance, the typical tremor (Event 4 in Figure 2) is likely located close to station B06, however, exhibits a long signal duration at B06, which may mainly reflect a long source process. Another feature is the depletion in high-frequency components (>10 Hz), which is observed even for the traces with short-duration signals (e.g., Figure 2b) and, thus, likely represents the critical feature for distinguishing tremors from ordinary earthquakes. Investigating whether a structural effect alone could also explain these features would be the first step toward addressing the above question. Furthermore, interactions between the surrounding structure and seismic source may occur. Although we have assumed a point source between the inclusions, a more realistic finite sized source could go through the inclusions to potentially affect the rupture process and duration. Investigation into these complicated cases will be the focus of future studies.

4.1. Definition of the Short-Duration Tremors in Comparison With LFEs

Deep (>15 km) tremors occasionally contain energetic and isolated pulses that have been identified as LFEs (Katsumata & Kamaya, 2003; Shelly, 2017). They are often considered as building blocks of tremors (Shelly et al., 2007; Figure 1d) and of the broadband slow earthquake phenomena (i.e., Brownian walk model) (Ide, 2008; Ide & Yabe, 2018). There are also reports on LFEs that are not associated with tremor signals (Arai et al., 2016; Aso et al., 2013; Nakajima & Hasegawa, 2021). Meanwhile, to date, LFEs have not been reported in association with shallow (<15 km) tremor signals. This fact raises a question of whether the short-duration tremors found at shallow depths and the LFEs could represent something similar that occurs at different depths.

LFEs are observed in a similar frequency range as tremors. In the above-mentioned studies, LFEs are defined as earthquakes with spectral power concentrated at 1–4 Hz or depleted in high-frequency components above ∼10 Hz. However, certain differences exist between LFEs and short-duration tremors. First, LFEs exhibit impulsive (i.e., short-duration) signals throughout the network up to approximately 30 km from the epicenter and do not become broadened like tremor signals, whereas the short-duration tremors exhibit short-duration signals only within approximately 10 km of the epicenter and exhibit broadened signals at farther distances. Second, LFE records preserve amplitude and phase information that reflects their seismic focal mechanism (Shelly et al., 2007). Conversely, the amplitude information reflecting their seismic radiation pattern is lost in the short-duration tremors (Figures 3b and 4d). Additionally, the phase information may be lost as explained in Figure S6 in Supporting Information S1. Some of these differences can be explained by the different source and receiver geometries (deep or shallow). Nevertheless, the LFEs that are not associated with tremor signals (e.g., Nakajima & Hasegawa, 2021) have been detected also at relatively shallow depths (<15 km), making it difficult to consider short-duration tremors as LFEs at shallow depths. Furthermore, Figure 3a shows that the short-duration tremors are likely end-members of tremors with varying source durations. They are not necessarily more energetic (i.e., not much larger in amplitude) compared to other tremors (Figures 2f–2h), while LFEs appear as energetic pulse and can be identified even with the long-lasting deep tremor signals in the background. Thus, based on current evidence, LFEs and short-duration tremors appear as different phenomena, however, this remains an open question.

Unlike what has been proposed for deep tremors, shallow tremors do not appear to contain the energetic and isolated processes in the middle of a long source process. Nevertheless, the Brownian walk model based on LFE observations (Ide, 2008) is not completely excluded as a possible tremor source model. This model considers diffusion as the primary process and, thus, does not require building blocks (i.e., LFEs or short-duration tremors) to emerge as isolated impulsive signals. The model is built on another important feature of tremors, that is, a very-low-frequency (VLF) signal (<0.1 Hz; Sugioka et al., 2012). Although VLF signals also accompanied tremors in the current study (Figure S7 in Supporting Information S1; To et al., 2015), they were not a primary focus of our analysis. Sugioka et al. (2012), who made the first close-in observations of VLF-tremors via broadband OBSs, interpreted the co-emergence VLF and tremor signals by slow shear failure and fluid-pressure-controlled tensile fractures. Thus, they proposed a two-modes rupture model. Our observations do not exclude their model either.

4.2. Toward Integrating Structures Observed at Different Scales

Our model appears consistent with a recently proposed geological structure for a tremor-source region. That is, Hirose et al. (2021) observed an upwelling mudflow from a borehole while drilling the shallowest part of a slow

earthquake fault zone in the Nankai trough, ~200 km southwest of our study region. The observation inferred that finite-sized overpressured aquifers to be patchily distributed in the fault zone. These aquifers likely have a significant contrast in permeability to the surroundings, thus, creating a large impedance contrast. Therefore, our proposed inclusions could be seismic expressions of these aquifers.

Furthermore, our findings may enable the integration of structures observed at different spatial scales. Based on seismic imaging, tremor source regions have been recognized as a low-velocity zone (Akuhara et al., 2020; Kamei et al., 2012; Park et al., 2010), and our results are consistent with this observation (Figure 4g). Small objects like inclusions are below the resolution of seismic imaging. Consequently, the images show macroscopic structures as a smoothed version of microscopic structures, such as inclusions, in space. Here we showed that seismic waves could become sensitive to objects smaller than their wavelength when the source is situated close by. As such, short-duration tremor records have the potential to connect structural observations at different scales, which would contribute to a better understanding of the cause of tremors.

4.3. Structure of Slow Earthquake Fault Zone

Our synthetic waveforms (Figures 4c and 4d) suggest that the differences between ordinary earthquakes and tremors may simply result from whether the seismic source is inside or outside the anomalous structure. Further, the form of fluids around the seismic source as relatively large-sized blobs, or aquifers, may account for the differences between the two phenomena. Furthermore, tremors are considered to share the same fault zone as other larger-sized slow earthquakes, such as VLF earthquakes and slow-slip events (Araki et al., 2017). Therefore, the unique medium around the tremor sources might be the structure along the slow earthquake fault zone, which could influence their source process.

5. Conclusions

We discovered short-duration tremors in OBS records obtained close to their source, suggesting that not all tremor sources are long. Based on current evidence, the short-duration tremors appear as a different phenomenon from previously reported LFEs. These observations further suggested that tremors' long signals comprise both source and structural effects. Using elastic wave propagation simulations, we showed that one possible structural model is a strongly scattering medium around a seismic source comprising many small low-velocity inclusions. These inclusions may represent the geologically detected aquifers in a tremor source region. Such a structure could be embedded along the slow earthquake fault zone and play a key role in their source process.

Data Availability Statement

The DONET1 data are available at National Research Institute for Earth Science and Disaster Resilience via doi.org/10.17598/NIED.0008. The spectral element program is available for download from gitlab.univ-nantes.fr/capdeville-y/spec2dya.

Acknowledgments
We thank an anonymous reviewer, Baoning Wu and Editor Germán Prieto for helpful comments to improve the manuscript. This work was supported by JSPS KAKENHI (19K04010, 20J40154, 21H05201) and MOST (111-2611-M-001-009). We drew figures using Generic Mapping Tools (Wessel et al., 2019) and Obspy (Beyreuther et al., 2010). The numerical simulations were performed at GLiCID Computing Centre, Pays de la Loire, France.

References

Akuhara, T., Tsuji, T., & Tonegawa, T. (2020). Overpressured underthrust sediment in the Nankai trough forearc inferred from transdimensional inversion of high-frequency teleseismic waveforms. *Geophysical Research Letters*, *47*(15), e2020GL088280. https://doi.org/10.1029/2020gl088280

Aoi, S., Asano, Y., Kunugi, T., Kimura, T., Uehira, K., Takahashi, N., et al. (2020). MOWLAS: NIED observation network for earthquake, tsunami and volcano. *Earth Planets and Space*, *72*(1), 126. https://doi.org/10.1186/s40623-020-01250-x

Arai, R., Takahashi, T., Kodaira, S., Kaiho, Y., Nakanishi, A., Fujie, G., et al. (2016). Structure of the tsunamigenic plate boundary and low-frequency earthquakes in the southern Ryukyu Trench. *Nature Communications*, *7*(1), 12255. https://doi.org/10.1038/ncomms12255

Araki, E., Saffer, D. M., Kopf, A. J., Wallace, L. M., Kimura, T., Machida, Y., et al. (2017). Recurring and triggered slow-slip events near the trench at the Nankai Trough subduction megathrust. *Science*, *356*(6343), 1157–1160. https://doi.org/10.1126/science.aan3120

Aso, N., Ohta, K., & Ide, S. (2013). Tectonic, volcanic, and semi-volcanic deep low-frequency earthquakes in western Japan. *Tectonophysics*, *600*(C), 27–40. https://doi.org/10.1016/j.tecto.2012.12.015

Beroza, G. C., & Ide, S. (2011). Slow earthquakes and non-volcanic tremor. *Annual Review of Earth and Planetary Sciences*, *39*(1), 271–296. https://doi.org/10.1146/annurev-earth-040809-152531

Beyreuther, M., Barsch, R., Krischer, L., Megies, T., Behr, Y., & Wassermann, J. (2010). ObsPy: A python toolbox for seismology. *Seismological Research Letters*, *81*(3), 530–533. https://doi.org/10.1785/gssrl.81.3.530

Bürgmann, R. (2018). The geophysics, geology and mechanics of slow fault slip. *Earth and Planetary Science Letters*, *495*, 112–134. https://doi.org/10.1016/j.epsl.2018.04.062

Chaljub, E., Komatitsch, D., Vilotte, J.-P., Capdeville, Y., Valette, B., & Festa, G. (2007). Spectral-element analysis in seismology. *Advances in Geophysics*, *48*, 365–419. https://doi.org/10.1016/s0065-2687(06)48007-9

Festa, G., & Vilotte, J. (2005). The newmark scheme as velocity–stress time-staggering: An efficient PML implementation for spectral element simulations of elastodynamics. *Geophysical Journal International*, *161*(3), 789–812. https://doi.org/10.1111/j.1365-246x.2005.02601.x

Hirose, T., Hamada, Y., Tanikawa, W., Kamiya, N., Yamamoto, Y., Tsuji, T., et al. (2021). High fluid-pressure patches beneath the décollement: A potential source of slow earthquakes in the Nankai Trough off Cape Muroto. *Journal of Geophysical Research: Solid Earth*, *126*(6), e2021JB021831. https://doi.org/10.1029/2021jb021831

Ide, S. (2008). A Brownian walk model for slow earthquakes. *Geophysical Research Letters*, *35*(17), L17301. https://doi.org/10.1029/2008gl034821

Ide, S. (2012). Variety and spatial heterogeneity of tectonic tremor worldwide. *Journal of Geophysical Research*, *117*(B3), 1–18. https://doi.org/10.1029/2011jb008840

Ide, S., Beroza, G. C., Shelly, D. R., & Uchide, T. (2007). A scaling law for slow earthquakes. *Nature*, *447*(7140), 76–79. https://doi.org/10.1038/nature05780

Ide, S., & Yabe, S. (2018). Two-dimensional probabilistic cell automaton model for broadband slow earthquakes. *Pure and Applied Geophysics*, *37*(10), 1–16. https://doi.org/10.1007/s00024-018-1976-9

Im, K., & Avouac, J.-P. (2021). Tectonic tremor as friction-induced inertial vibration. *Earth and Planetary Science Letters*, *576*, 117238. https://doi.org/10.1016/j.epsl.2021.117238

Kamei, R., Pratt, R. G., & Tsuji, T. (2012). Waveform tomography imaging of a megasplay fault system in the seismogenic Nankai subduction zone. *Earth and Planetary Science Letters*, *317–318*, 343–353. https://doi.org/10.1016/j.epsl.2011.10.042

Kaneda, Y., Kawaguchi, K., Araki, E., Matsumoto, H., Nakamura, T., Kamiya, S., & Takahashi, N. (2015). Seafloor observatories, a new vision of the Earth from the abyss. In P. Favali, L. Beranzoli, & A. D. Santis (Eds.), (pp. 643–663). *Springer praxis books*.

Katsumata, A., & Kamaya, N. (2003). Low-frequency continuous tremor around the Moho discontinuity away from volcanoes in the southwest Japan (pp. 1–4). https://doi.org/10.1029/2002gl0159812

Komatitsch, D., & Vilotte, J.-P. (1998). The spectral element method: An efficient tool to simulate the seismic response of 2D and 3D geological structures. *Bulletin of the Seismological Society of America*, *2*(88), 368–392. https://doi.org/10.1785/bssa0880020368

Nakajima, J., & Hasegawa, A. (2021). Prevalence of shallow low-frequency earthquakes in the continental crust. *Journal of Geophysical Research: Solid Earth*, *126*(4), e2020JB021391. https://doi.org/10.1029/2020jb021391

Nakano, M., Nakamura, T., & Kaneda, Y. (2015). Hypocenters in the Nankai Trough determined by using data from both ocean-bottom and land seismic networks and a 3D velocity structure model: Implications for seismotectonic activity. *Bulletin of the Seismological Society of America*, *105*(3), 1594–1605. https://doi.org/10.1785/0120140309

Obana, K., & Kodaira, S. (2009). Low-frequency tremors associated with reverse faults in a shallow accretionary prism. *Earth and Planetary Science Letters*, *287*(1–2), 168–174. https://doi.org/10.1016/j.epsl.2009.08.005

Park, J. O., Fujie, G., Wijerathne, L., Hori, T., Kodaira, S., Fukao, Y., et al. (2010). A low-velocity zone with weak reflectivity along the Nankai subduction zone. *Geology*, *38*(3), 283–286. https://doi.org/10.1130/g30205.1

Park, J.-O., Moore, G. F., Tsuru, T., Kodaira, S., & Kaneda, Y. (2003). A subducted oceanic ridge influencing the Nankai megathrust earthquake rupture. *Earth and Planetary Science Letters*, *217*(1–2), 77–84. https://doi.org/10.1016/s0012-821x(03)00553-3

Saffer, D. M., & Wallace, L. M. (2015). The frictional, hydrologic, metamorphic and thermal habitat of shallow slow earthquakes. *Nature Geoscience*, *8*(8), 594–600. https://doi.org/10.1038/ngeo2490

Shelly, D. R. (2017). A 15 year catalog of more than 1 million low-frequency earthquakes: Tracking tremor and slip along the deep San Andreas Fault. *Journal of Geophysical Research: Solid Earth*, *122*(5), 3739–3753. https://doi.org/10.1002/2017JB014047

Shelly, D. R., Beroza, G. C., & Ide, S. (2007). Non-volcanic tremor and low-frequency earthquake swarms. *Nature*, *446*(7133), 305–307. https://doi.org/10.1038/nature05666

Sibson, R. (2017). Tensile overpressure compartments on low-angle thrust faults. *Earth Planets and Space*, *69*(1), 1–15. https://doi.org/10.1186/s40623-017-0699-y

Sugioka, H., Okamoto, T., Nakamura, T., Ishihara, Y., Ito, A., Obana, K., et al. (2012). Tsunamigenic potential of the shallow subduction plate boundary inferred from slow seismic slip. *Nature Geoscience*, *5*(6), 414–418. https://doi.org/10.1038/ngeo1466

Takemura, S., Yabe, S., & Emoto, K. (2020). Modelling high-frequency seismograms at ocean bottom seismometers: Effects of heterogeneous structures on source parameter estimation for small offshore earthquakes and shallow low-frequency tremors. *Geophysical Journal International*, *223*(3), 1708–1723. https://doi.org/10.1093/gji/ggaa404

To, A., Obana, K., Sugioka, H., Araki, E., Takahashi, N., & Fukao, Y. (2015). Small size very low frequency earthquakes in the Nankai accretionary prism, following the 2011 Tohoku-Oki earthquake. *Physics of the Earth and Planetary Interiors*, *245*(C), 40–51. https://doi.org/10.1016/j.pepi.2015.04.007

Toh, A., Obana, K., & Araki, E. (2018). Distribution of very low frequency earthquakes in the Nankai accretionary prism influenced by a subducting-ridge. *Earth and Planetary Science Letters*, *482*, 342–356. https://doi.org/10.1016/j.epsl.2017.10.062

Ueno, H., Hatakeyama, S., Aketagawa, T., Funasaki, J., & Hamada, N. (2002). *Improvement of hypocenter determination procedures in the Japan Meteorological Agency* (pp. 1–12). The Seismological Society of Japan. Retrieved from https://www.data.jma.go.jp/svd/eqev/data/bulletin/data/hypo/relocate.html

Wessel, P., Luis, J. F., Uieda, L., Scharroo, R., Wobbe, F., Smith, W. H. F., & Tian, D. (2019). The generic mapping tools version 6. *Geochemistry, Geophysics, Geosystems*, *20*(11), 5556–5564. https://doi.org/10.1029/2019gc008515

Zhao, M., Capdeville, Y., & Zhang, H. (2016). Direct numerical modeling of time-reversal acoustic subwavelength focusing. *Wave Motion*, *67*, 102–115. https://doi.org/10.1016/j.wavemoti.2016.07.010

References From the Supporting Information

Burgos, G., Capdeville, Y., & Guillot, L. (2016). Homogenized moment tensor and the effect of near-field heterogeneities on nonisotropic radiation in nuclear explosion. *Journal of Geophysical Research: Solid Earth*, *121*(6), 4366–4389. https://doi.org/10.1002/2015JB012744

Tamaribuchi, K., Kobayashi, A., Nishimiya, T., Hirose, F., & Annoura, S. (2019). Characteristics of shallow low-frequency earthquakes off the Kii Peninsula, Japan, in 2004 revealed by ocean bottom seismometers. *Geophysical Research Letters*, *46*(23), 13737–13745. https://doi.org/10.1029/2019GL085158

Yabe, S., & Ide, S. (2014). Spatial distribution of seismic energy rate of tectonic tremors in subduction zones. *Journal of Geophysical Research: Solid Earth*, *119*(11), 8171–8185. https://doi.org/10.1002/2014JB011383